

Selective Hydrogenation of Nitriles to Imines Over a Multifunctional Heterogeneous Pt Catalyst

Jilan Long, Bialin Yin, and Yingwei Li

Key Laboratory of Fuel Cell Technology of Guangdong Province, School of Chemistry and Chemical Engineering, South China University of Technology, Guangzhou 510640, China

Lianjie Zhang

Key Laboratory of Specially Functional Materials of MoE, Inst. of Polymer Optoelectronic Materials & Devices, South China University of Technology, Guangzhou 510640, China

DOI 10.1002/aic.14545

Published online July 5, 2014 in Wiley Online Library (wileyonlinelibrary.com)

Imines and their derivatives are versatile synthetic intermediates for the industrial preparation of both bulk and fine chemicals and for pharmaceuticals, but preparing these compounds efficiently through direct hydrogenation of nitriles are hindered by overhydrogenation to secondary amines. Here we report a highly efficient multifunctional catalyst system for selective hydrogenation coupling of nitriles to secondary imines using a heterogeneous Pt catalyst that was deposited on a nickel-based metal-organic framework (MOF) containing DABCO. The catalyst showed excellent synergy in promoting the hydrogenation of a variety of nitriles, giving significantly improved activity and selectivity (up to >99% yield) even under atmospheric pressure of H₂. It is suggested that the Lewis base (DABCO) sites on the Ni-MOF inhibit further hydrogenation of the imines. The influence of H₂ pressure, reactant concentration, stirring speed, and reaction temperature was investigated. The kinetics and mechanism of hydrogenation of benzonitrile (BN) by the Pt/Ni-MOF catalyst has been studied. The reaction showed a first-order dependence on both BN concentration and H₂ pressure. A kinetic model was proposed based on the mechanism of nitriles hydrogenation and compared with experimental observations. © 2014 American Institute of Chemical Engineers AICHE J, 60: 3565–3576, 2014

Keywords: heterogeneous catalysis, hydrogenation, imines, metal-organic frameworks, nitriles

Introduction

Imines and their derivatives are versatile synthetic intermediates that have been extensively utilized for synthesis of dyes, fragrances, fungicides, pharmaceuticals, and agricultural chemicals.^{1–3} In general, there are presently three commonly utilized approaches for imines synthesis, that is, condensation of amines with ketones or aldehydes (Figure 1, path A),⁴ oxidative self-coupling of amines (path B),^{5–10} and oxidative coupling of amines with alcohols (path C).^{11–21} From a practical point of view, the use of amines as raw materials would significantly limit the widespread application of these methods because amines are normally expensive.²² Moreover, most of these catalytic systems suffer from important drawbacks regarding the production of large amount of unwanted by-products, limited substrates compatibility, and/or difficulty for reuse.^{23–25} In these regards, the development of a highly efficient, green, and sustainable catalytic methodology for imine synthesis still remains a great challenge to date.

Nitriles are usually readily available as bulk chemicals, and more importantly they are inexpensive relative to amines. Additionally, the catalytic hydrogenation of nitriles represents an atom-economic and valuable route to amines, although most of the systems require harsh reaction conditions to achieve a high yield of amines.^{26–28} Therefore, as for the synthesis of imines, the direct hydrogenation of nitriles to imines is highly desirable, which could represent a step forward toward green, economic, and sustainable processes (Figure 1, path D). However, the selective catalytic hydrogenation of nitriles to form imines is challenging due to the easy overhydrogenation of imines to secondary amines (Figure 2).^{29–33} Compared to the substantial work being done on imines synthesis using amines as starting materials, to the best of our knowledge, so far only two reports have described the direct hydrogenation of nitriles to imines.^{34,35} Moreover, the reported protocols all use homogeneous phosphorus-containing organometallic complexes [e.g., bipyridine-based PNN Ru(II) pincer complex] as catalysts, and show a restricted scope of substrates as well as relatively low yields. The homogeneous systems are unstable and not significant environmentally friendly, because the catalysts are difficult to be separated from the products and recycled, which is a particular drawback for applications in the pharmaceutical and food industry. In this regard, heterogeneous catalysts are a promising solution to these problems, because

Additional Supporting Information may be found in the online version of this article.

Correspondence concerning this article should be addressed to Y. Li at liyw@scut.edu.cn.

© 2014 American Institute of Chemical Engineers

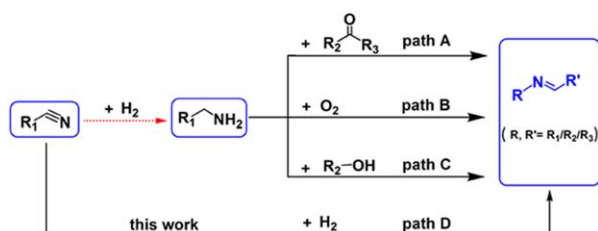


Figure 1. Methodologies for the preparation of imine.

[Color figure can be viewed in the online issue, which is available at wileyonlinelibrary.com.]

these materials can be readily separated from the reaction mixture and reused.³⁶

In view of these settings, there is clearly a need to develop heterogeneous catalysts for selective hydrogenation of nitriles to imines that have greatly enhanced catalytic efficiency as well as wide substrates compatibility. Herein, we report the direct hydrogenation coupling of nitriles to imines over a novel heterogeneous platinum catalyst, which is deposited on a nickel-containing metal-organic framework (denoted by Ni-MOF) with a formula unit of $[\text{Ni}_2(\text{bdc})_2(\text{DABCO})]$ (bdc = terephthalate, DABCO = 1,4-diazabicyclo[2.2.2]octane) (Figure 3a).^{37–39} The rational design of the Pt/Ni-MOF catalyst is mainly based on the following considerations. First, in the Ni-MOF, the coordination of nickel is unsaturated, which could have a strong interaction with nitrile and promote the initial hydrogenation of nitrile to form a primary imine and further hydrogenation to generate an amine intermediate. The presence of basic DABCO moieties might facilitate the addition reaction between the formed amine and primary imine to produce the desired secondary imine product. Conversely, to slow down further hydrogenation of the formed imine, platinum is selected as the hydrogenation active species because of its weaker hydrogenation ability relative to palladium or ruthenium.^{40,41} The multifunctional catalyst system showed excellent synergy in selective hydrogenation of a variety of nitriles to imines, giving significantly improved activity and selectivity. The reaction could even be carried out effectively at hydrogen pressures as low as atmospheric pressure, and >99% conversion of nitrile was observed with >99% selectivity to imine.

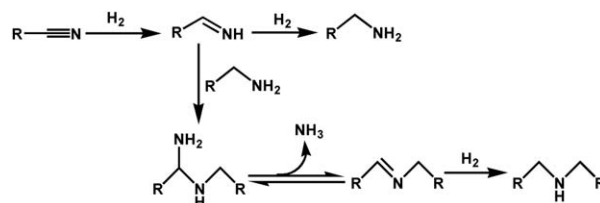


Figure 2. Reaction network in the hydrogenation of nitriles.

Experimental

Chemicals

All chemicals were purchased from commercial sources and used without further treatments. All solvents were analytical grade and distilled prior to use.

Catalyst preparation and characterization

Ni-MOF was prepared and purified according to the reported procedures.^{37–39} Ni-MOF supported Pt catalysts were prepared by using a colloidal deposition method. Typically, a methanol solution of H_2PtCl_6 (10^{-3} M) was first prepared with polyvinylpyrrolidone (PVP) as protecting agent (PVP monomer/Pt = 10:1, molar ratio). The mixture was vigorously stirred for 1 h in an ice bath (0°C). A freshly prepared methanol solution of NaBH_4 (0.1 M, $\text{NaBH}_4/\text{Pt} = 5:1$, molar ratio) was injected rapidly to the solution. The color of the mixture immediately turned from pale yellow to brown. The pH of the solution was kept at around 7–8. Within a few minutes of sol generation, the desolvent Ni-MOF was added to the colloidal solution and stirred for 6 h, followed by washing thoroughly with methanol. The sample was dried under vacuum at 100°C for 2 h and then was treated in a stream of H_2 at 200°C for 2 h to yield Pt/Ni-MOF.

For comparison, various materials including Ni-MOF-74 ($1308 \text{ m}^2/\text{g}$), activated carbon ($1039 \text{ m}^2/\text{g}$), and Al_2O_3 ($59 \text{ m}^2/\text{g}$), were also used as support for Pt or Pt-Ni nanoparticles (NPs). The supported Pt catalysts (0.8 wt % Pt) were prepared by using the same recipes as described earlier for the synthesis of Pt/Ni-MOF. For the preparation of Pt-Ni catalysts [Pt, 0.8 wt %; Pt:Ni = 1:1.4 (molar ratio)], a solution of H_2PtCl_6 and $\text{Ni}(\text{NO}_3)_2$ with PVP (PVP monomer/metal = 10:1, molar ratio) was first prepared using methanol (for activated carbon) or deionized water (for Al_2O_3) as solvent.

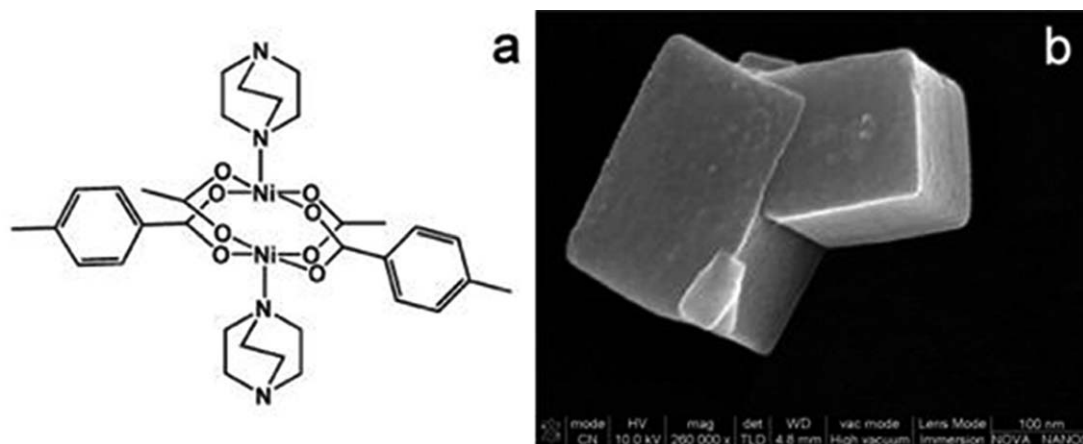


Figure 3. Schematic illustration of the structure of Ni-MOF (a) and representative SEM image of the as-synthesized MOF crystals (b).

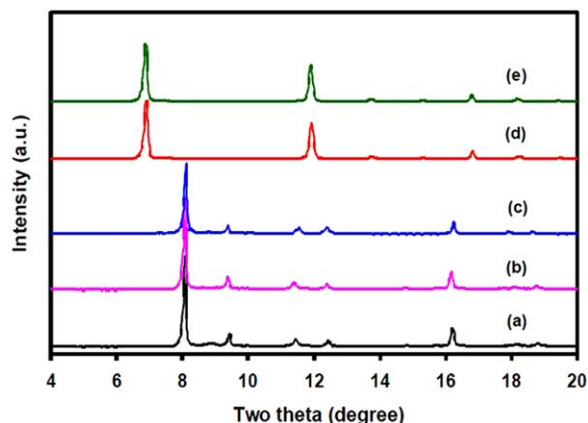


Figure 4. Powder XRD patterns of the MOF samples: (a) Ni-MOF (as-synthesized); (b) 0.8%Pt/Ni-MOF before catalytic reaction; (c) 0.8%Pt/Ni-MOF after catalytic reaction; (d) Ni-MOF-74; and (e) Pt/Ni-MOF-74.

[Color figure can be viewed in the online issue, which is available at [wileyonlinelibrary.com](http://www.wileyonlinelibrary.com).]

Powder X-ray diffraction patterns of the samples were recorded on a Rigaku diffractometer (D/MAX-III A, 3 kW) using Cu K α radiation (40 kV, 30 mA, 0.1543 nm). Brunauer, Emmert, and Teller (BET) surface area and pore sizes were obtained from N₂ adsorption/desorption isotherms at 77 K with a Micromeritics ASAP 2020M instrument. Before measurements, the samples were degassed at 100°C overnight. The metal loadings of the samples were measured quantitatively by atomic absorption spectroscopy (AAS) on a Hitachi Z-2300 instrument. The size and morphology of the samples were investigated by using a transmission electron microscope (TEM, JEOL, JEM-2010HR) with energy-dispersive X-ray spectroscopy analysis. Prior to analysis, the solids were suspended in ethanol and deposited straight away on a copper grid. X-ray photoelectron spectroscopy (XPS) measurements were performed on a Kratos Axis Ultra DLD system with a base pressure of 10^{−9} Torr. The basic property was determined by CO₂-TPD measured by the pulse technique on a Micromeritics AutoChem II 2920 instrument. Typically, 60 mg of activated sample was pretreated under a flow of Argon (30 mL min^{−1}) at 300°C for 3 h. Then, the sample was cooled to 100°C under a flow of Ar. After adsorption of CO₂, the sample was purged in Ar flow at 100°C. The TPD data were collected from 100°C to 300°C at a heating rate of 10°C min^{−1} in a flow of Argon.

Catalytic reactions

The hydrogenation of nitrile was carried out in a 15 mL autoclave with a polytetrafluoroethylene liner. The autoclave was sealed and purged several times with pure H₂ to remove the air after the addition of nitrile, solvent, and catalyst. Then, the H₂ pressure was adjusted to 0.8 MPa, and the reactor was loaded into an oil bath that was preheated to 100°C. The stirring speed was about 800 r/min. After reaction, the reactor was cooled to room temperature. The identity of the products was verified by gas chromatography (GC)–mass spectrum (MS), the yields of the products and conversion of nitriles were determined by GC with diphenyl ether as an internal standard.

For the recyclability test, the Pt/Ni-MOF catalyst was separated from the reaction mixture by centrifugation after reaction, thoroughly washed with ethyl acetate and methanol,

dried at 100°C under high vacuum, and then was reused as catalyst for the next run.

Results and Discussion

Characterization results

Scanning Electron Microscope (SEM) images of the as-synthesized Ni-MOF showed regular cuboid crystals of approximately 100–200 nm in dimensions (Figure 3b). The powder XRD patterns (Figure 4) of the Ni-MOF matched well with those reported in literature,^{37–39} confirming the MOF structure of the prepared material in this work. After loading Pt NPs, the framework of Ni-MOF was mostly maintained (Figure 4). Moreover, no diffractions were detected for platinum NPs, which indicated Pt NPs were too small in all samples. The doping amount of Pt on the MOF was around 0.8 wt %, on the basis of AAS analysis. TEM images of the 0.8%Pt/Ni-MOF showed that the Pt NPs dispersed uniformly on the MOF, with particle sizes typically between 2 and 3 nm (mean size: 2.51 ± 0.66 nm) (Figure 5). XPS spectra of the Pt/Ni-MOF sample (Figure 6) showed that the binding energies of the Pt 4f_{7/2} and Pt 4f_{5/2} peaks were 71.5 and 74.8 eV, respectively, confirming the efficient reduction of Pt(IV) to Pt(0).⁴²

The stability of the porous structure of Ni-MOF before and after metal doping could be further confirmed by N₂ adsorption experiments at 77 K (Supporting Information Figure S1). The BET specific surface area was 1737 and 1160 m²/g for Ni-MOF and Pt/Ni-MOF, respectively. The obvious decrease in N₂ adsorption amount might be due to the blockage of cavities of Ni-MOF by Pt NPs located in the micropores or at the surface of the MOF network. As can be seen from the pore-size distribution curves (Supporting Information Figure S1), the modification of Ni-MOF with Pt NPs led to a slight decrease in the pore sizes of the MOF.

The basic property of the Ni-MOF was determined by CO₂-TPD. In general, the strength of basic sites may be determined from CO₂ desorption temperatures. The higher desorption temperature, the stronger basicity.^{43,44} A broad peak showed in the CO₂-TPD profile for the Ni-MOF at a temperature lower than 300°C proved that the Ni-MOF contained some weak basic sites (Supporting Information Figure S2), indicating that there were some uncoordinated nitrogen atoms of DABCO on the surface of the MOF. The presence of such uncoordinated groups (e.g., carboxylate) of the organic ligands in MOFs has also been observed in other reports.⁴⁵

Catalytic hydrogenation of benzonitrile: Optimization of reaction conditions

The blank run of benzonitrile (BN) hydrogenation was carried out at 100°C and 5 MPa H₂, which gave essentially no activity (even with the parent Ni-MOF) in the systems after 10 h of reaction (Table 1, entries 1 and 2). Initially, we doped Ni-MOF with Pd because Pd catalysts have been widely used in the hydrogenation of nitriles to amines.^{46–48} No desired imine product (i.e., *N*-benzylidene-1-phenylmethanamine [BDMA]) was detected when using 0.8 wt % Pd/Ni-MOF as catalyst, suggesting that the use of Pd catalyst easily led to overhydrogenation and the formation of secondary amine (i.e., dibenzylamine [DBA]).

To overcome the problem of overhydrogenation, we doped Ni-MOF with Pt, which is known having weaker

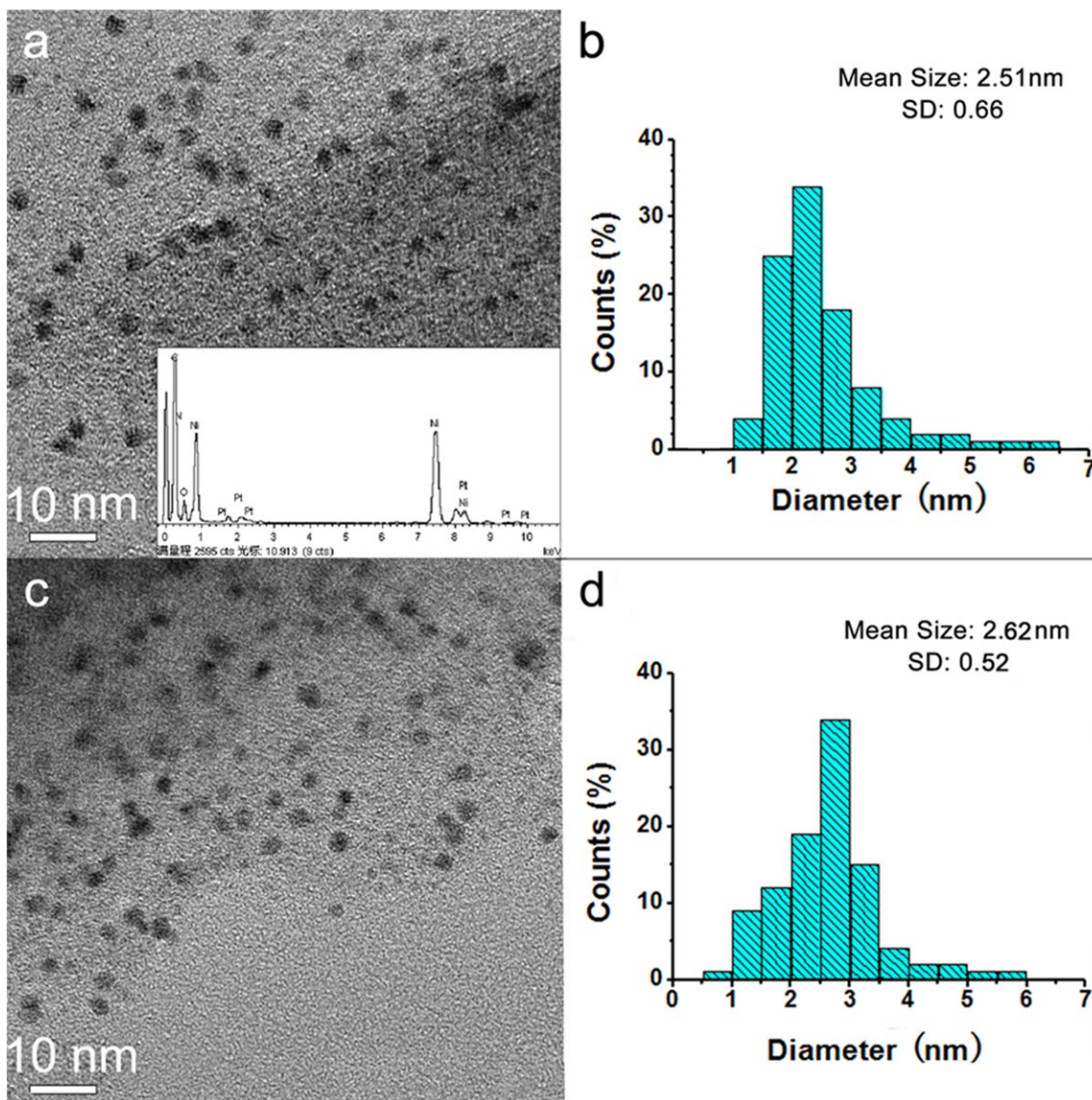


Figure 5. TEM images of 0.8%Pt/Ni-MOF before (a) and after catalytic reaction (c), and the corresponding size distribution of Pt NPs (b, and d).

The inset in (a) is the EDX pattern. [Color figure can be viewed in the online issue, which is available at wileyonlinelibrary.com.]

hydrogenation ability relative to Pd. As shown in Table 1, the reaction with 0.8 wt % Pt/Ni-MOF as catalyst generated imine (BDMA) as the only product without the detection of any amines products (DBA and 1-phenylmethanamine) at 100°C and 2 MPa of H₂ after 2 h of reaction (entry 3).

Using the 0.8 wt % Pt/Ni-MOF catalyst, a further optimization of the reaction parameters was subsequently conducted. Prolonging the reaction time enhanced the conversion of BN (Table 1, entry 4), but which also resulted in significant production of the secondary amine DBA, that is, the overhydrogenation product. The H₂ pressure and reaction temperature were found to strongly influence the reaction. Decreasing the pressure from 2 to 0.5 MPa remarkably enhanced the selectivity to imine while retaining a high conversion of BN at 100°C (Figure 7). Nevertheless, an increase in temperature led to a decrease in the selectivity to imine due to the overhydrogenation (Figure 8). The selectivity toward DBA was about 95% with only a trace amount of the desired imine (BDMA) produced in the reaction at 0.8 MPa when temperature was increased to 150°C (Figure 8).

Given these initial promising results, we investigated the effect of the amount of solvent on the hydrogenation. Decreasing the quantity of solvent affected the conversion and selectivity, reducing the selectivity of BDMA to 96% with the formation of about 4% of overhydrogenation product at 0.8 MPa and 100°C after 10 h of reaction (Table 1, entries 5–6). The overhydrogenation could be effectively inhibited by lowering the reaction temperature to 80°C (entry 7). Under the optimized conditions, we investigated the effect of metal content and proved that 0.8 wt % Pt was the best catalyst in the hydrogenation of BN to BDMA (Table 1, entries 7–9). The lower hydrogenation activity observed over the 1.2 wt % Pt catalyst might be due to the aggregation of Pt NPs on the Ni-MOF support (Supporting Information Figure S3).

Using the 0.8 wt % Pt/Ni-MOF as catalyst, we further investigated the hydrogenation at lower pressures. Although a decrease in H₂ pressure led to a reduced conversion, the reaction could be fully restored, simply by prolonging the reaction time, and/or enhancing the temperature (entries 10–11). Notably, the reaction proceeded with a selectivity of >99% to

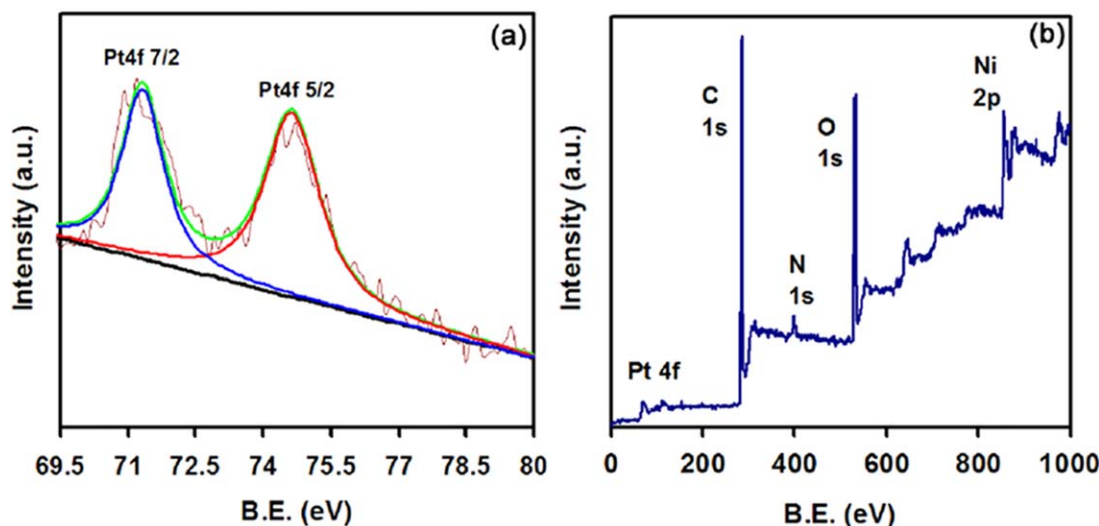


Figure 6. XPS spectra of 0.8%Pt/Ni-MOF: (a) Pt 4f and (b) survey spectra.

[Color figure can be viewed in the online issue, which is available at wileyonlinelibrary.com.]

BDMA at a complete conversion, even at atmospheric pressure of H_2 (entry 12). To the best of our knowledge, such a high activity (with >99% selectivity at the same time) in the hydrogenation of nitriles to imines at atmospheric pressure has not been reported to date. The reaction also proceeded smoothly at a high substrate/metal molar ratio (1500:1), affording a quantitative yield of imine after prolonging the reaction time (entry 13). It is noteworthy that the reaction also proceeded very well at 1-g scale, further demonstrating the synthetic utility of our catalyst system (entry 14).

Reusability of the Pt/Ni-MOF catalyst

In a further set of experiments, we investigated the recyclability of the Pt/Ni-MOF catalyst, because it is crucial to confirm that the highly active catalyst can be reused.

Results included in Table 1 indicate that no efficiency loss was observed in the BN hydrogenation up to five runs (Supporting Information Figure S4). The crystalline structure of Ni-MOF was mostly retained after catalytic reactions (Figure 4). TEM images of the recycled catalyst showed no significant aggregation of Pt particles (average size: 2.62 ± 0.52 nm) in the material (Figure 5). Moreover, the reaction was stopped after 0.5 h and the liquid mixture was carefully removed by hot filtration. AAS analysis indicated that no metal had leached into the liquid phase during reaction. The liquid phase after removing the catalyst did not exhibit any further reactivity (Figure 9). These results demonstrated the stability and reusability of the highly active Pt/Ni-MOF catalyst under the investigated conditions.

Table 1. Results of the Hydrogenation of Benzonitrile^a

							Selectivity (%) ^b		
Entry	Catalyst	Time (h)	P_{H_2} (MPa)	T (°C)	Con. (%) ^b		PMA	DBA	BDMA
1	—	10	5	100	—	—	—	—	—
2	Ni-MOF	10	5	100	—	—	—	—	—
3	Pt/Ni-MOF	2	2	100	69	—	—	—	>99
4	Pt/Ni-MOF	10	2	100	98	—	—	37	63
5	Pt/Ni-MOF	10	0.8	100	92	—	—	—	>99
6 ^c	Pt/Ni-MOF	10	0.8	100	>99	—	—	4	96
7 ^c	Pt/Ni-MOF	10	0.8	80	>99	—	—	—	>99
8 ^{c,d}	Pt/Ni-MOF	10	0.8	80	85	—	—	—	>99
9 ^{c,e}	Pt/Ni-MOF	10	0.8	80	98	—	—	—	>99
10 ^c	Pt/Ni-MOF	10	0.2	80	35	—	—	—	>99
11 ^c	Pt/Ni-MOF	35	0.2	80	>99	—	—	—	>99
12 ^c	Pt/Ni-MOF	35	0.1	100	>99	—	—	—	>99
13 ^{c,f}	Pt/Ni-MOF	20	0.8	80	>99	—	—	—	>99
14 ^g	Pt/Ni-MOF	30	0.8	80	>99	—	—	—	>99

^aConditions: 0.8 wt % Pt/Ni-MOF, benzonitrile (1.5 mmol), substrate: Pt = 200 (mole ratio), toluene (2 mL).

^bThe conversions and selectivities were determined by GC with diphenyl ether as an internal standard.

^cToluene (1 mL).

^d1.2 wt % Pt/Ni-MOF as catalyst.

^e0.4 wt % Pt/Ni-MOF as catalyst.

^fSubstrate: Pt = 1500 (molar ratio).

^gSubstrate: Pt = 1500 (molar ratio), benzonitrile (10 mmol), toluene (5 mL).

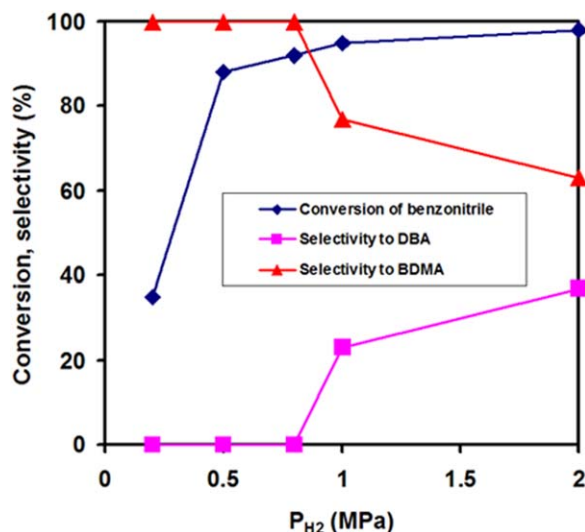


Figure 7. Effect of reaction pressure on the hydrogenation of BN over the Pt/Ni-MOF catalyst.

Reaction conditions: BN (1.5 mmol), substrate: Pt = 200 (mole ratio), toluene (2 mL), 100°C, 10 h. [Color figure can be viewed in the online issue, which is available at wileyonlinelibrary.com.]

Reaction mechanism for the hydrogenation of nitriles to imines over Pt/Ni-MOF

In view of these findings, we have proposed a plausible reaction mechanism for the hydrogenation coupling of nitriles to imines over Pt/Ni-MOF. As shown in Figure 3, the nickel ion in the Ni-MOF is five-coordinated, which could still have a coordination interaction with the nitrogen atom of the BN molecule because the coordination number of Ni is normally six. It is well known that platinum clusters are capable of dissociating activation of H_2 molecules (Figure 10, II).^{49,50} The dissociated H atoms then diffuse over the MOF surface by spillover to reach the adsorbed

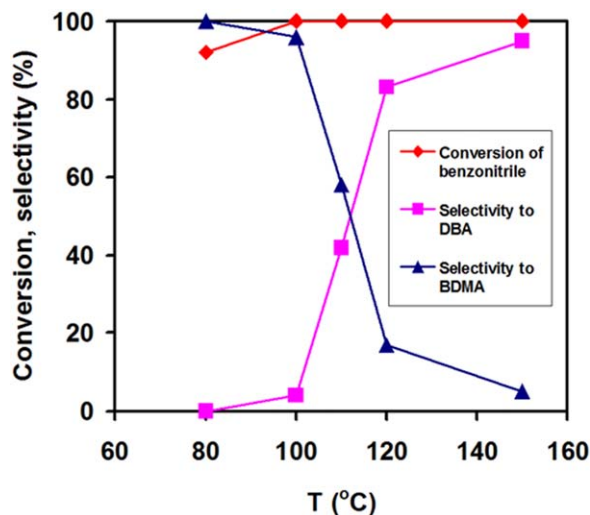


Figure 8. Effect of reaction temperature on the hydrogenation of BN over the Pt/Ni-MOF catalyst.

Reaction conditions: BN (1.5 mmol), substrate: Pt = 200 (mole ratio), toluene (2 mL), H_2 (0.8 MPa), 10 h. [Color figure can be viewed in the online issue, which is available at wileyonlinelibrary.com.]

nitrile molecule,^{51–53} hydrogenating the $C\equiv N$ bond to form a primary imine intermediate (Figure 10, III), which is very active and can be further hydrogenated to produce a primary amine.^{35,54–56} The Lewis base (DABCO) site could obtain a proton from amine to form the intermediate V.^{57,58} Subsequently, the deprotonated amine reacts with the primary imine intermediate III by nucleophilic attack, simultaneously with a proton transfer from DABCO to give the intermediate VI,^{4,54–58} which liberates a diamine with regeneration of the catalyst.⁵⁶ Finally, NH_3 liberation from the diamine generates the desired secondary imine product.^{4,54–56}

Inhibition of further hydrogenation of secondary imines is suggested as a crucial factor underlying the excellent selectivity to imines that we observed over the Pt/Ni-MOF catalyst. To investigate the effect of the Lewis base (DABCO) sites on the hydrogenation, we conducted the hydrogenation of BN under the optimized conditions using Pt/Ni-MOF-74 as the catalyst (Supporting Information Tables S1). Ni-MOF-74 is also a Ni-containing MOF with a formula unit of $[Ni_2(DHBDC)]$ (DHBDC = 2,5-dihydroxy-1,4-benzene-dicarboxylate) (Supporting Information Figure S5), while has no DABCO units.^{59,60} When using the 0.8 wt % Pt/Ni-MOF-74 catalyst, DBA was observed as the predominant product in the hydrogenation of BN (Supporting Information Tables S1, entry 2). However, the reaction produced the desired BDMA in quantitative yield when a small amount of DABCO (0.25 mmol) was added with Pt/Ni-MOF-74 (Supporting Information Tables S1, entry 3). The results suggest that the uncoordinated DABCO sites on the surface of the Ni-MOF suppressed the overhydrogenation effectively.

To further demonstrate the significance of the use of the Ni-MOF support in promoting the formation of imine, we also prepared Pt or Pt-Ni catalysts supported on traditional supports, for example, activated carbon and Al_2O_3 . The hydrogenation results under the optimized conditions (Supporting Information Table S1) indicated that all these catalysts tended to overhydrogenate to the secondary amine. Pt-Ni bimetallic nanoparticles supported on carbon or Al_2O_3 obtained higher conversions of BN than those with Pt alone

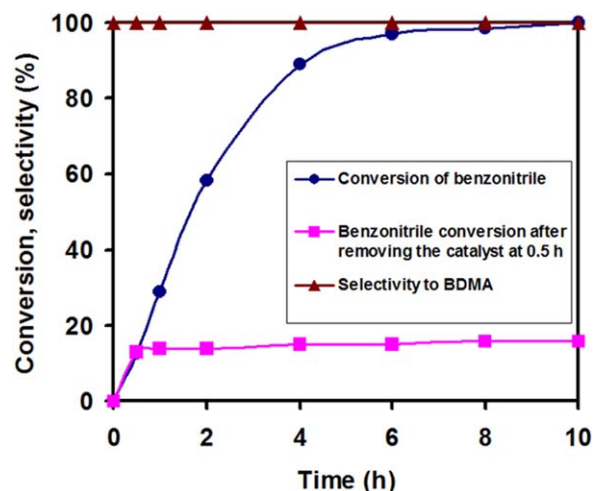


Figure 9. BN conversion and BDMA selectivity as a function of time: BN (1.5 mmol), substrate: Pt = 200 (molar ratio), toluene (1 mL), H_2 (0.8 MPa), 80°C.

[Color figure can be viewed in the online issue, which is available at wileyonlinelibrary.com.]

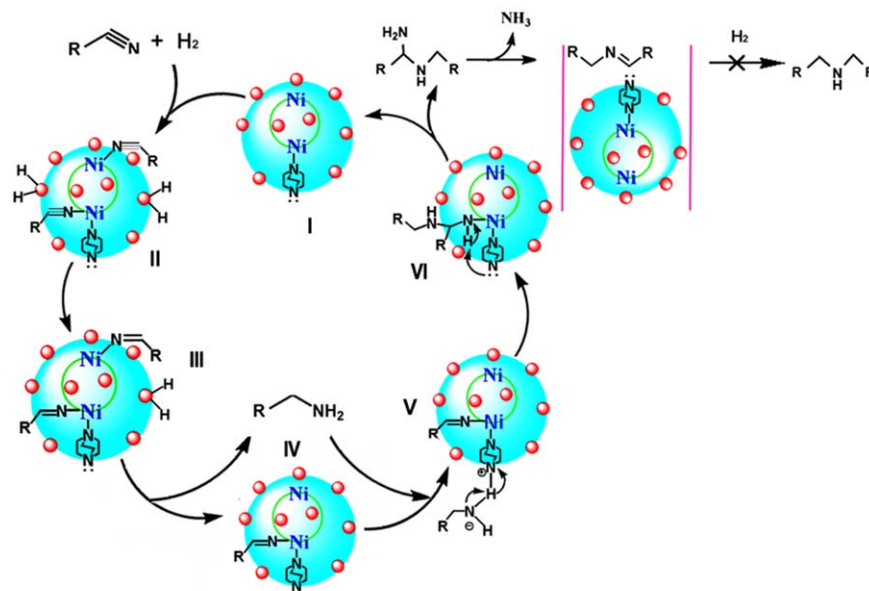


Figure 10. Plausible pathways for hydrogenation coupling of nitriles over Pt/Ni-MOF.

[Color figure can be viewed in the online issue, which is available at [wileyonlinelibrary.com](http://www.interscience.wiley.com).]

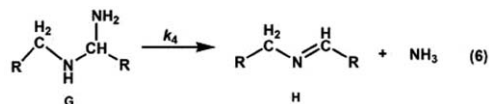
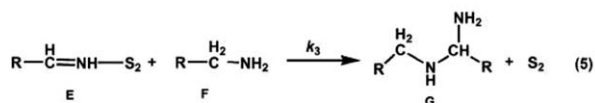
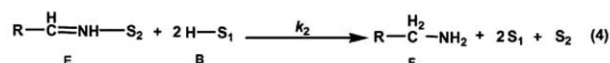
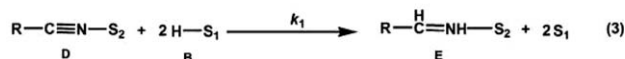
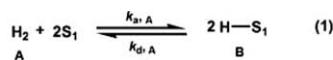
but could not inhibit the further hydrogenation of imine. It was found that the addition of a small amount of DABCO (0.25 mmol) to the Pt-Ni/C system significantly improved the selectivity to the desired imine (Supporting Information Table S1, entries 5 and 6). From the above results obtained on the catalysts using different supports, it could be concluded that the use of the particular Ni-MOF support is significant for achieving a high catalytic efficiency in the hydrogenation of nitriles to imines (without the addition of DABCO in the reaction solution).

We also investigated the effect of DABCO addition on the catalytic performance of Pt/Ni-MOF. The conversion/selectivity versus time data (Supporting Information Figure S6) indicated that the addition of different amounts of DABCO up to 2 mmol did not affect BN conversion and BDMA selectivity significantly, suggesting that the amount of DABCO in the Ni-MOF could be sufficient to promote the formation of imines under the condition.

To further confirm this finding, we carried out the experiments of imine (BDMA) hydrogenation under identical conditions (Supporting Information Table S2). Only trace amount of the hydrogenation product, that is DBA, was observed over the Pt/Ni-MOF catalyst (Supporting Information Table S2, entry 1). However, the hydrogenation of BDMA gave about 60% conversion over the Pt/Ni-MOF-74 (Supporting Information Table S2, entry 2). To account for this phenomenon, we investigated the interaction between BDMA and DABCO by theoretic calculation. The structure of the complex formed by BDMA and DABCO is found at DFT-M06-2X/6-31G(d,p) level⁶¹ and depicted in Supporting Information Figure S7. This complex is stabilized by the intermolecular interaction between N atom in DABCO and C=N double bond in BDMA. The stabilization energy of this complex is 19.2 kJ/mol (ΔH_{298K}) that suggests there exists a moderate strong interaction between the Lewis basic DABCO and the C=N in imine. We believe that this interaction inhibited further hydrogenation of imine over Pt/Ni-MOF.

Kinetics model for the hydrogenation of nitriles to imines over Pt/Ni-MOF

Based on the mechanism sketched in Figure 10, the reaction steps of the hydrogenation can be written as



where S_1 is the Pt site on the catalyst, and S_2 is the Ni ion in the Ni-MOF.

As can be seen from the obtained experimental results in the hydrogenation of BN over the Pt/Ni-MOF catalyst, the intermediates E, F, and G were never detected in the reaction mixture. Therefore, it could be speculated that these species were very active and thus underwent the further reactions (Steps 4–6) very quickly. Assuming hydrogenation of adsorbed nitrile to primary imine to be the rate determining step (Step 3), the reaction rate is described by

$$r = k_1 [\text{D}] [\text{B}]^2$$

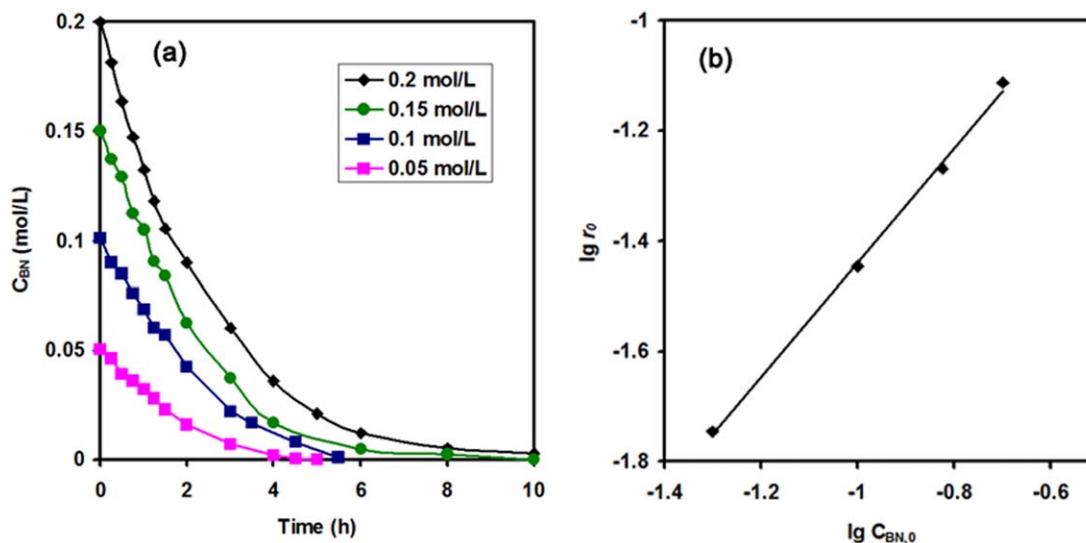


Figure 11. BN concentration as a function of time for four different initial BN concentration (a) and plot of $\lg r_0$ versus $\lg C_{BN,0}$ (b).

Reaction conditions: H_2 (0.8 MPa), $80^\circ C$. [Color figure can be viewed in the online issue, which is available at wileyonlinelibrary.com.]

where $[B]$ is the surface concentration of hydrogen on site S_1 , and k_1 is the rate constant for the addition of two H atoms to the nitrile. The assumption of quasi-equilibrated H_2 adsorption on S_1 sites yields the following expression for surface concentration of H_2

$$K_A = \frac{[B]^2}{[A][S_1]^2} \quad \left(K_A = \frac{k_{a,A}}{k_{d,A}} \right)$$

$$[B]^2 = K_A [A] [S_1]^2$$

where $[A]$ is the liquid-phase concentration of H_2 . According to the Henry's law, $[A] = P_A \times H$ (H is a constant), so

$$[B]^2 = K_A H [S_1]^2 P_A$$

$$[B]^2 = K_H [S_1]^2 P_A \quad (K_H = K_A H)$$

Analogously, quasi-equilibrated nitrile (C) adsorption on S_2 sites yields

$$K_C = \frac{[D]}{[C][S_2]} \quad \left(K_C = \frac{k_{a,C}}{k_{d,C}} \right)$$

$$[D] = K_C [C] [S_2]$$

Combining the preceding equations gives the following rate expression:

$$r = k_1 [D] [B]^2 = k_1 \times K_C [C] [S_2] \times K_H [S_1]^2 P_A$$

$$= k_1 K_C K_H [S_1]^2 [S_2] [C] P_A$$

Assuming that the adsorption of H_2 and nitrile on catalyst is weak adsorption, $[S_1]$ and $[S_2]$ can be considered as constants. Lumping constants together we get finally

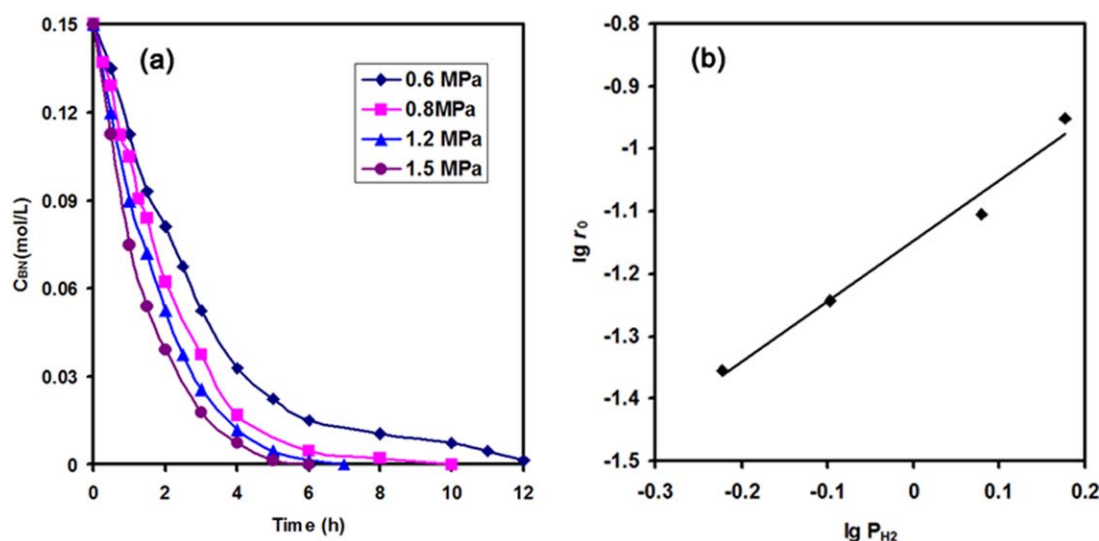


Figure 12. BN concentration as a function of time for four different H_2 pressure (a) and plot of $\lg r_0$ versus $\lg P_{H_2}$ (b).

Reaction conditions: BN (1.5 mmol), $80^\circ C$. [Color figure can be viewed in the online issue, which is available at wileyonlinelibrary.com.]

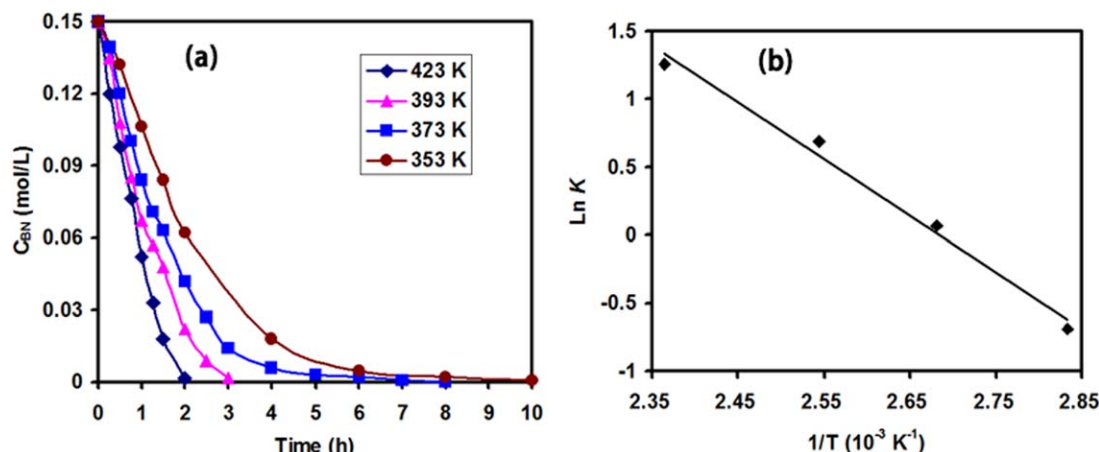


Figure 13. BN concentration as a function of time for four different temperature (a) and the Arrhenius plot (b).

Reaction conditions: BN (1.5 mmol), H₂ (0.8 MPa). [Color figure can be viewed in the online issue, which is available at wileyonlinelibrary.com.]

$$r = k[C]P_A$$

with

$$k = k_1 K_C K_H [S_1]^2 [S_2]$$

Effect of stirring speed on the catalytic performance of Pt/Ni-MOF

Since the stirring speed is a crucial factor for the external mass transfer of a liquid-phase catalytic reaction, and could control the total reaction rate, the hydrogenation of BN over the Pt/Ni-MOF catalyst under different stirring rates was investigated. The reactions were conducted at 80°C and 0.8 MPa of H₂, and the results are presented in Supporting Information Figure S8. The conversion of BN increased when the stirring speed was enhanced from 300 to 600 r/min. However, no apparent changes in reaction rate were observed at stirring speeds higher than 600 r/min, indicating that the stirring rate was sufficiently high for negligible gas–liquid mass-transfer effect.

Effect of initial BN concentration on the catalytic hydrogenation

Kinetic experiments were conducted over the 0.8 wt % Pt/Ni-MOF catalyst at the following conditions: 80°C, 0.8 MPa, BN concentrations of 0.05, 0.1, 0.15, and 0.2 M. Plot of BN concentrations versus time is shown in Figure 11a. It can be seen that increasing the initial BN concentrations ($C_{BN,0}$) enhanced the reaction rates. It is noteworthy that there was no other product except the secondary imine (BDMA) formed in the reactions under different initial BN concentrations. Thus, the highest yield of BDMA was obtained at the time of complete conversion of BN for each initial BN concentration.

Table 2. Rate Constants for Benzonitrile Hydrogenation at Four Temperatures

T (K)	k ($10^{-3} \text{ h}^{-1} \text{ MPa}^{-1}$)
353	0.501
373	1.069
393	1.989
423	3.507

From the concentrations versus time curves, the reaction rate (r_0) at each initial concentration could be determined. Plot of $\lg r_0$ versus $\lg C_{BN,0}$ (Figure 11b) shows that $\lg r_0$ is a linear function of $\lg C_{BN,0}$. The slope of the straight line for the four BN concentrations was about 1.03. This result indicates that the reaction was first-order dependence on BN concentrations, which is in good agreement with the theoretic kinetics model shown above.

Effect of H₂ pressure on the hydrogenation of BN

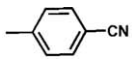
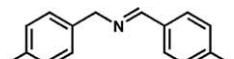
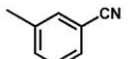
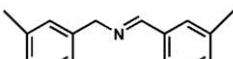
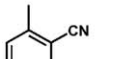
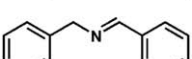
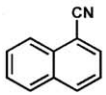
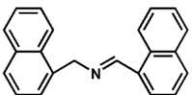
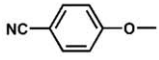
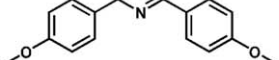
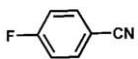
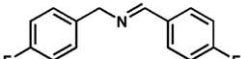
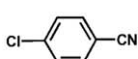
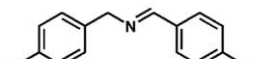
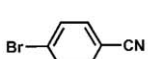
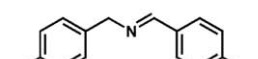
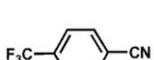
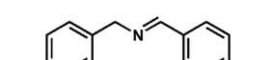
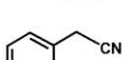
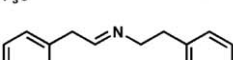
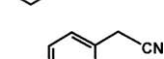
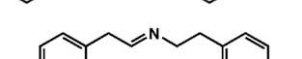





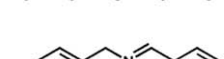
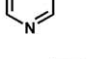
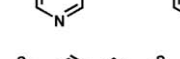
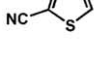

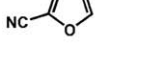

The effects of H₂ pressure on BN conversions are summarized in Figure 12a at the following conditions: 80°C, BN concentration of 0.15 M, and H₂ pressure of 0.6, 0.8, 1.2, and 1.5 MPa. Thus, we see that increasing the H₂ pressure increased the reaction rate, reducing the time needed to attain the completion of BN conversion. Likewise, the selectivity to the desired secondary imine (BDMA) was 100% for each run up to the complete conversion of BN.

Figure 12b presents $\lg r_0$ versus $\lg P_{H_2}$ with the initial reaction rates determined from the time evolution of the BN concentration for each run shown in Figure 12a. The plot shows that $\lg r_0$ is a linear function of $\lg P_{H_2}$. The slope of the line for the four H₂ pressures was about 0.98, suggesting that the reaction was first-order dependence on H₂ pressure, in accordance with the theoretic kinetics model.

Effect of reaction temperature on the hydrogenation of BN

Figure 13a shows the concentrations of BN versus time for temperatures of 80, 100, 120, and 150°C at 0.8 MPa of H₂ using Pt/Ni-MOF as catalyst. Because the rate of reaction increased with temperature, the time to achieve complete conversion of BN dropped considerably with increasing temperature, as expected. For example, the time to reach the maximum conversion was about 8 h at 100°C but only 2 h at 150°C. Up to the completion of BN conversion, secondary imine (BDMA) was the only product detected in the reaction. But after that time a further reaction would lead to overhydrogenation to secondary amine (DBA). Therefore, the highest yield of BDMA was achieved at the time of just reaching a complete conversion of BN for each reaction temperature.

Table 3. Hydrogenation of Various Nitriles^a

Entry	Substrate	Time (h)	Product	Yield (%) ^b
1		30		98
2		30		97
3		30		97
4 ^{b,c}		30		95
5		30		>99
6		30		98
7		30		99
8		30		98
9		30		97
10		30		98
11		30		96
12		8		95
13 ^{c,d}		8		90
14 ^{c,d}		72		88
15 ^{c,d}		72		90
16 ^{c,d}		72		95
17 ^{c,d}		72		>99

^aSubstrate: Pt = 1500 (molar ratio), substrate (1.5 mmol), 0.8 MPa H₂, 80°C, toluene (1 mL).^bGC yield.^cSubstrate: Pt = 750 (molar ratio).^dReaction temperature: 100°C.

According to the rate expression shown above, we could obtain the rate constants at the four temperatures (Table 2). If the rate constants follow the Arrhenius expression

$$\ln k = \ln A - \frac{E_a}{RT}$$

In k should be a linear function of $1/T$. Figure 13b shows a typical Arrhenius plot for hydrogenation of BN at 0.8 MPa over Pt/Ni-MOF. From this plot, the activation energy and pre-exponential factor were determined from the slope and intercept of the straight line for the four temperatures covered, which was about 34.6 kJ/mol, and $7.2 \times 10^4 \text{ h}^{-1} \text{ MPa}^{-1}$, respectively.

Hydrogenation of various nitriles to imines

In a final set of experiments, we investigated the scope of nitriles amenable to be converted into imines via the newly developed Pt/Ni-MOF catalyzed hydrogenation protocol. BNs substituted with electron-donating groups, such as methyl and methoxyl, underwent the hydrogenation reaction smoothly to afford the corresponding imines in excellent yields (Table 3, entries 1–5). Notably, even the highly sterically hindered *o*-tolunitrile and 1-naphthonitrile could also be efficiently hydrogenated to give the imines products in 90–97% yields (entries 3 and 4) at 80°C, 0.8 MPa of H₂, and a substrate/metal molar ratio of 1500:1. Likewise the hydrogenation of electron poor BNs, such as 4-fluorobenzonitrile, 4-chlorobenzonitrile, and 4-bromobenzonitrile, all proceeded well and furnished the desired imines in almost quantitative yields (entries 6–9). Importantly, the halide moieties were intact under the conditions, which would offer an opportunity to further functionalize the products.

The catalytic system was also adapted for the hydrogenation of aliphatic nitriles (Table 3, entries 10–13). Phenylacetoneitrile, 4-bromophenylacetoneitrile, and even linear alkyl nitriles such as valeronitrile and hexanenitrile, were successfully hydrogenated to give the corresponding imines in excellent yields.

Finally, the performance of the Pt/Ni-MOF catalyst was investigated in the hydrogenation of heterocyclic nitriles, which are known as challenging substrates that might deactivate the metal catalysts due to their chelating nature.³⁵ Here, low yields to the desired imines were observed in the reduction of substituted furans, thiophenes, and pyridines. However, by slightly increasing the reaction temperature to 100°C while decreasing the ratio of substrate to Pt meal to 750:1, the corresponding products could be formed in good to excellent yields (Table 3, entries 14–16). Furthermore, dinitrile could also be selectively hydrogenated at one nitrile group to give the corresponding imine in quantitative yield (entry 17). The inhibition of further hydrogenation of the yielded secondary imine at the nitrile moieties might be attributed to a steric hindrance effect of the micropores of Ni-MOF (Supporting Information Figure S1).

Conclusions

In summary, we have successfully developed a novel and highly efficient multifunctional catalyst system for selective hydrogenation of nitriles to imines using a heterogeneous platinum catalyst that is dispersed on a nickel-based MOF containing DABCO. The catalyst shows excellent synergy in the hydrogenation of a variety of nitriles, giving significantly improved activity and selectivity even under atmospheric pressure of H₂. Coordination with the Ni ion in MOF promotes the activation of nitrile, while Pt activates H₂. The dangling basic DABCO linkers on the MOF surface facilitate the addition reaction between the formed amine and primary imine to produce the desired secondary imine product. At the same time, coordination interaction between DABCO and secondary imine inhibits further hydrogenation to amine. The reaction shows a first-order dependence on both BN concentration and H₂ pressure. A kinetics model has been proposed based on the mechanism of nitriles hydrogenation and compared with experimental observations. This novel synthetic strategy for fabrication of high-performance multifunctional catalysts might open new perspectives for the

application of the emerging MOF materials in selective catalysis processes.

Acknowledgments

This work was supported by NSF of China (20936001, 21322606, and 21073065), Doctoral Fund of Ministry of Education of China (20120172110012), Guangdong NSF (S2011020002397 and 10351064101000000), and the Fundamental Research Funds for the Central Universities (2013ZG0001).

Literature Cited

1. Hadjipavlou-Litina DJ, Geronikaki AA. Thiazolyl and benzothiazolyl Schiff bases as novel possible lipooxygenase inhibitors and anti inflammatory agents. Synthesis and biological evaluation. *Drug Des Discov*. 1998;15:199–206.
2. Adams JP. Imines, enamines and oximes. *J Chem Soc Perkin Trans. I* 2000;2:125–139.
3. Rappoport Z, Liebman JF. The Chemistry of Hydroxylamines, Oximes and Hydroxamic Acids. New York: Wiley, 2009:609–635.
4. Gnanaprakasam B, Zhang J, Milstein D. Direct synthesis of Imines from alcohols and amines with liberation of H₂. *Angew Chem Int Ed*. 2010;49:1468–1471.
5. Huang H, Huang J, Liu YM, He HY, Cao Y, Fan KN. Graphite oxide as an efficient and durable metal-free catalyst for aerobic oxidative coupling of amines to imines. *Green Chem*. 2012;14:930–934.
6. Patil RD, Adimurthy S. Copper-catalyzed aerobic oxidation of amines to imines under neat conditions with low catalyst loading. *Adv Synth Catal*. 2011;353:1695–1700.
7. Patil RD, Adimurthy S. Copper(0)-catalyzed aerobic oxidative synthesis of imines from amines under solvent-free conditions. *RSC Adv*. 2012;2:5119–5122.
8. Liu L H, Wang ZK, Fu XF, Yan CH. Azobisisobutyronitrile initiated aerobic oxidative transformation of amines: coupling of primary amines and cyanation of tertiary amines. *Org Lett*. 2012;14:5692–5695.
9. Chu GB, Li CB. Convenient and clean synthesis of imines from primary benzylamines. *Org Biomol Chem*. 2010;8:4716–4719.
10. Bosanac T, Wilcox CS. Precipiton reagents: precipiton phosphines for solution-phase reductions. *Org Lett*. 2004;6:2321–2324.
11. Gunanathan C, Milstein D. Metal ligand cooperation by aromatization dearomatization: a new paradigm in bond activation and “green” catalysis. *Acc Chem Res*. 2011;44:588–602.
12. Xu J, Zhuang RQ, Bao LL, Tang G, Zhao YF. KOH-mediated transition metal-free synthesis of imines from alcohols and amines. *Green Chem*. 2012;14:2384–2387.
13. Kang Q, Zhang YG. Copper-catalyzed highly efficient aerobic oxidative synthesis of imines from alcohols and amines. *Green Chem*. 2012;14:1016–1019.
14. Shiraishi Y, Ikeda M, Tsukamoto D. One-pot synthesis of imines from alcohols and amines with TiO₂ loading Pt nanoparticles under UV irradiation. *Chem Commun*. 2011;47:4811–4813.
15. Jiang L, Jin LL, Tian HW, Yuan XQ, Yu XC, Xu Q. Direct and mild palladium-catalyzed aerobic oxidative synthesis of imines from alcohols and amines under ambient conditions. *Chem Commun*. 2011;47:10833–10835.
16. Tian HW, Yu XC, Li Q, Wang JX, Xu Q. General, green, and scalable synthesis of imines from alcohols and amines by a mild and efficient copper-catalyzed aerobic oxidative reaction in open air at room temperature. *Adv Synth Catal*. 2012;354:2671–2677.
17. Zhang GQ, Hanson SK. Cobalt-catalyzed acceptorless alcohol dehydrogenation: synthesis of imines from alcohols and amines. *Org Lett*. 2013;15:650–653.
18. Esteruelas MA, Honczek N, Oliván M, Oñate E, Valencia M. Direct access to POP-type osmium(ii) and osmium(iv) complexes: osmium a promising alternative to ruthenium for the synthesis of imines from alcohols and amines. *Organometallics* 2011;30:2468–2471.
19. Sun H, Su FZ, Ni J, Cao Y, He HY, Fan K. Gold supported on hydroxyapatite as a versatile multifunctional catalyst for the direct tandem synthesis of imines and oximes. *Angew Chem Int Ed*. 2009;48:4390–4393.
20. Kegnæs S, Mielby J, Mentzel UV, Christensen CH, Riisager A. Formation of imines by selective gold-catalysed aerobic oxidative

- coupling of alcohols and amines under ambient conditions. *Green Chem.* 2010;12:1437–1441.
21. Milstein D. Discovery of environmentally benign catalytic reactions of alcohols catalyzed by pyridine-based pincer Ru complexes, based on metal–ligand cooperation. *Top Catal.* 2010;53:915–923.
 22. Huang J, Yu L, He L, Liu YM, Cao Y, Fan KN. Direct one-pot reductive imination of nitroarenes using aldehydes and carbon monoxide by titania supported gold nanoparticles at room temperature. *Green Chem.* 2011;13:2672–2677.
 23. Blackburn L, Taylor RJK. In situ oxidation-imine formation-reduction routes from alcohols to amines. *Org Lett.* 2001;3:1637–1639.
 24. Kwon MS, Kim S, Park S, Bosco W, Chidrala RK, Park J. One-pot synthesis of imines and secondary amines by Pd-catalyzed coupling of benzyl alcohols and primary amines. *J Org Chem.* 2009;74:2877–2879.
 25. Kim JW, He J, Yamaguchi K, Mizono N. Heterogeneously catalyzed one-pot synthesis of aldimines from primary alcohols and amines by supported ruthenium hydroxides. *Chem Lett* 2009;38:920–921.
 26. Ullmann F. *Ullmann's Encyclopedia of Industrial Chemistry*. Weinheim: WILEY-VCH Verlag, 1985:167–180.
 27. Enthaler S, Addis D, Junge K, Erre G, Beller M. A general and environmentally benign catalytic reduction of nitriles to primary amines. *Chem Eur J.* 2008;14:9491–9494.
 28. Haddenham D, Pasumansky L, DeSoto J, Eagon S, Singaram B. Reductions of aliphatic and aromatic nitriles to primary amines with diisopropylaminoborane. *J Org Chem.* 2009;74:1964–1970.
 29. Gomez S, Peters JA, Maschmeyer T. The reductive amination of aldehydes and ketones and the hydrogenation of nitriles: mechanistic aspects and selectivity control. *Adv Synth Catal.* 2002;344:1037–1057.
 30. DK, Palit BK, Saha CR. Dihydrogen reduction of organic substrates using orthometallated ruthenium (II) complex catalysts. *J Mol Catal A: Chem.* 1994;88:57–70.
 31. Chin CS, Lee B. Hydrogenation of nitriles with iridium-triphenylphosphine complexes. *Catal Lett.* 1992;14:135–140.
 32. Galan A, Mendoza J, Prados P, Rojo J, Echavaren AM. Synthesis of secondary amines by rhodium catalyzed hydrogenation of nitriles. *J Org Chem.* 1991;56:452–454.
 33. Rajesh K, Dudge B, Blacque O, Berke H. Homogeneous hydrogenations of nitriles catalyzed by rhenium complexes. *Adv Synth Catal.* 2011;353:1479–1484.
 34. Silva PZ, Solar IJ, Crestani MG, Arévalo A, Francisco RB, García JJ. Catalytic hydrogenation of aromatic nitriles and dinitriles with nickel compounds. *Appl Catal A: Gen.* 2009;363:230–234.
 35. Srimani D, Feller M, David YB, Milstein D. Catalytic coupling of nitriles and amines to form imines under mild hydrogen pressure. *Chem Commun.* 2012;48:11853–11855.
 36. Kundu SK, Mondal J, Bhaumik A. Tungstic acid functionalized mesoporous SBA-15: A novel heterogeneous catalyst for facile one-pot synthesis of 2-amino-4H-chromenes in aqueous medium. *Dalton Trans.* 2013;42:10515–10524.
 37. Dybtsev DN, Chun H, Kim K. Rigid and flexible: a highly porous metal–organic framework with unusual guest-dependent dynamic behavior. *Angew Chem Int Ed.* 2004;43:5033–5036.
 38. Lee JY, Olson DH, Pan L, Emge TJ, Li J. Microporous metal–organic frameworks with high gas sorption and separation capacity. *Adv Funct Mater.* 2007;17:1255–1262.
 39. Tan K, Nijem N, Canepa P, Gong Q, Li J, Thonhauser T, Chabal YJ. Stability and hydrolyzation of metal organic frameworks with paddle-wheel sub upon hydration. *Chem Mater.* 2012;24:3153–3167.
 40. Sun J, Karim AM, Zhang H, Kovarik L, Li XS, Hensley AJ, McEwen JS, Wang Y. Carbon-supported bimetallic Pd–Fe catalysts for vapor-phase hydrodeoxygenation of guaiacol. *J Catal.* 2013;306:47–57.
 41. Mortensen PM, Grunwaldt JD, Jensen PA, Jensen AD. Screening of catalysts for hydrodeoxygenation of phenol as a model compound for bio-oil. *ACS Catal.* 2013;3:774–1785.
 42. Fleisch TH, Zajac GW, Schreiner JO, Mains GJ. An XPS study of the UV photoreduction of transition and noble metal oxides. *Appl Surf Sci.* 1986;26:488–497.
 43. Mandala S, Santra C, Bando KK, Jamesa OO, Maity S, Mehtad D, Chowdhury B. Aerobic oxidation of benzyl alcohol over mesoporous Mn-doped ceria supported Au nanoparticle catalyst. *J Mol Catal A: Chem.* 2013;378:47–56.
 44. Dieuzeide ML, Jobbagy M, Amadeo N. Glycerol steam reforming over Ni γ -Al₂O₃ catalysts. modified with Mg(II). Effect of Mg (II) content. *Catal Today.* 2013;213:50–57.
 45. Park TH, Hickman AJ, Koh K, Martin S, Wong-Foy AG, Sanford MS, Matzger AJ. Highly dispersed palladium(II) in a defective metal–organic framework: application to C–H activation and functionalization. *J Am Chem Soc.* 2011;133:20138–20141.
 46. Hegedüs L, Máthé T. Selective heterogeneous catalytic hydrogenation of nitriles to primary amines in liquid phase: Part I. Hydrogenation of benzonitrile over palladium. *Appl Catal A: Gen* 2005;296:209–215.
 47. Chatterjee M, Ishizaka T, Suzuki T, Suzuki A, Kawanami H. In situ synthesized Pd nanoparticles supported on B-MCM-41: an efficient catalyst for hydrogenation of nitroaromatics in supercritical carbon dioxide. *Green Chem.* 2012;14:3415–3422.
 48. Foubister AJ, Brown, GR. Direct transformation of cyano into methyl groups under mild conditions. *Synthesis.* 1982;12:1036–1037.
 49. Kohn HW, Boudart M. Reaction of hydrogen with oxygen adsorbed on a platinum catalyst. *Science.* 1964;145:149–150.
 50. Triwahyono S, Yamada T, Hattori H. Kinetic study of hydrogen adsorption on Pt/WO₃-ZrO₂ and WO₃-ZrO₂. *Appl Catal A: Gen.* 2003;250:65–73.
 51. Li YW, Yang RT. Significantly enhanced hydrogen storage in metal–organic frameworks via spillover. *J Am Chem Soc.* 2006;128:726–727.
 52. Li YW, Yang RT. Communication hydrogen storage in metal–organic frameworks by bridged hydrogen spillover. *J Am Chem Soc.* 2006;128:8136–8137.
 53. Li YW, Yang FH, Yang RT. Kinetics and mechanistic model for hydrogen spillover on bridged metal–organic frameworks. *J Phys Chem C.* 2007;111:3405–3411.
 54. Al-Hmoud L, Jones CW. Reaction pathways over copper and cerium oxide catalysts for direct synthesis of imines from amines under aerobic conditions. *J Catal.* 2013;301:116–124.
 55. Werkmeister S, Bornschein C, Junge K, Beller M. Selective ruthenium-catalyzed transfer hydrogenations of nitriles to amines with 2-butanol. *Chem Eur J.* 2013;19:4437–4440.
 56. Reguillo R, Grellier M, Vautravers N, Vendier L, Etienne SS. Ruthenium-catalyzed hydrogenation of nitriles: insights into the mechanism. *J Am Chem Soc.* 2010;132:7854–7855.
 57. Shinde S, Rashinkar G, Salunkhe R. DABCO entrapped in agar-agar: a heterogeneous gelly catalyst for multi-component synthesis of 2-amino-4H-chromenes. *J Mol Liq.* 2013;178:122–126.
 58. Bangade VM, Reddy BC, Thakur PB, Babu BM, Meshram HM. DABCO catalyzed highly regioselective synthesis of fused imidazo-heterocycles in aqueous medium. *Tetrahedron Lett.* 2013;54:4767–4771.
 59. Rosi NL, Kim J, Eddaoudi M, Chen BL, O'Keeffe M, Yaghi OM. Rod packings and metal–organic frameworks constructed from rod-shaped secondary building units. *J Am Chem Soc.* 2005;127:1504–1518.
 60. Caskey SR, Wong-Foy AG, Matzger AJ. Dramatic tuning of carbon dioxide uptake via metal substitution in a coordination polymer with cylindrical pores. *J Am Chem Soc.* 2008;130:10870–10871.
 61. Zhao Y, Truhlar DG. The M06 suite of density functionals for main group thermochemistry, thermochemical kinetics, noncovalent interactions, excited states, and transition elements: two new functionals and systematic testing of four M06-class functionals and 12 other functionals. *Theor Chem Acc.* 2008;120:215–241.

Manuscript received Mar. 23, 2014, and revision received June 12, 2014.